PHYSICS

Quantum electronics and optics

EXPERIMENTAL VERIFICATION OF THE GOUY PHASE FOR HIGHER-ORDER HERMITE–GAUSSIAN BEAMS

**Lyubomir Stoyanov, Nasko Gorunski, Maria Mincheva,
Petko Drenkov, Edmon Lazarov, Alexander Dreischuh**✉

Abstract

The Gouy phase is related to the axial phase shift experienced by any focused light beam with respect to a reference plane wave when passing through its focus. Generally, the Gouy phase Φ_G for a higher-order Hermite–Gaussian (HG) beam is this for the fundamental Gaussian beam multiplied by a factor, which is the sum of the mode indices of the HG beam plus unity. Although this result is a paradigm in optics, we are not aware of its experimental verification. In this paper, we present experimental results obtained with a single-lens interferometer for higher-order HG modes generated using spatial light modulator. The retrieved Gouy phase Φ_G is found in a very good quantitative agreement with the mentioned theoretical result.

Key words: laser modes, Hermite–Gaussian mode, Gouy phase

1. Introduction. It is known that any focused light beam experiences an axial phase shift with respect to a reference plane wave when passing through its focus. This phase anomaly was first studied by Gouy and is named after him. The chronology of early studies can be found in [1]. Later, most of the research

was related to the development of microwave optics, lasers, nonlinear optics, terahertz radiation, and singular optics, just to mention a few. Let us denote by L_D and z the Rayleigh diffraction length of a Gaussian beam and the longitudinal coordinate, respectively. Then, the Gouy phase for a Gaussian beam is given by $\Phi_G = \arctan(z/L_D)$. For a higher-order Hermite–Gaussian (HG) mode with mode indices (l, m) this phase is multiplied by a factor of $(1 + l + m)$ [2]. In other words, passing through the focal plane, higher-order Hermite–Gaussian modes accumulate a higher Gouy phase $\Phi_G = (1 + l + m) \arctan(z/L_D)$ with respect to a reference fundamental Gaussian beam. The Gouy phase has important consequences in, e.g., nonlinear optics. In general, the n-th order nonlinear polarization will experience a phase shift that is n times larger than that experienced by the pump wave [3,4]. It is natural to expect that the Gouy phase also has profound consequences in highly nonlinear processes like above-threshold ionization [5] and high-harmonic generation [6].

One relatively intuitive example for the Gouy phase is based on the confocal laser cavity emitting a fundamental Gaussian beam. It is known (see, e.g., [7, Chap. 4.7.2]) that in such a cavity, at the waist of the beam, the wavefront is flat. However, at the planes of the mirrors, it is spherical (concave to the left/right mirror, respectively), exactly matching the curvatures of the corresponding mirrors. Hence, at its axis the Gaussian beam is accumulating additional phase (the Gouy phase) in comparison to a (infinite) plane wave.

Equally intuitive is the single-lens interferometer, a device remarkably frugal and insensitive to laser beam fluctuations, suitable for measuring phase changes. We successfully exploited it to measure the Gouy phase of higher-order Hermite–Gaussian beams. However, since it is not a commonly used instrument, we will briefly describe its action in the experimental section of this paper.

Even though the cases of a fundamental Gaussian beam are relatively well-studied, we are not aware of any experimental data published in the literature confirming the dependence $\Phi_G = (1 + l + m) \arctan(z/L_D)$ for the higher-order HG_{lm} modes. One very distant exception is the use of the Hermite–Gaussian mode HG_{01} and a pair of cylindrical lenses for mode conversion outside the laser cavity [8]. In this paper, we present analytical model and experimental results obtained with a single-lens interferometer. Information on the Gouy phase Φ_G for higher-order Hermite–Gaussian modes is retrieved. The data are in very good quantitative agreement with the mentioned theoretical result.

2. Derivation of the Gouy phase for Hermite–Gaussian beams. Let us briefly derive the analytical result for the Gouy phase $\Phi_G(z)$ of higher-order Hermite–Gaussian beam (HGB). We follow the approach described in [2]. The longitudinal evolution of the Gouy phase $\Phi_G(z)$ can be calculated from the transverse components k_x and k_y of the wavenumber k using the relation

$$(1) \qquad \Phi_G = -\frac{1}{k} \int \left(\langle k_x^2 \rangle + \langle k_y^2 \rangle \right) \, dz.$$

Let us define the field amplitude of HGB as

$$(2) \qquad f_{l,m}(x,y) = \sqrt{\frac{2C(l,m)}{\pi\omega^2(z)}} H_l\left(\frac{\sqrt{2}x}{\omega(z)}\right) H_m\left(\frac{\sqrt{2}y}{\omega(z)}\right) \exp\left[-\frac{x^2+y^2}{\omega^2(z)}\right],$$

where the (Gaussian) beam width $\omega(z)$ at a particular distance z is related to its width $\omega_0(z=0)$ at the beam waist (at $z=0$) by $\omega^2(z) = \omega_0^2[1+(z/z_R)^2]$. Here $z_R = \pi\omega_0^2/\lambda$ is the Rayleigh diffraction range and λ is the wavelength. $C(l,m)$ is a normalization factor ensuring that the beam intensity is equal to unity for all mode indices (l,m) of the Hermite polynomials H_l and H_m. Using the orthogonality between Hermite polynomials, it can be shown that $C(l,m) = 1/(2^l l! 2^m m!)$.

According to [2, Eq. 7], the angular spectrum $\widetilde{F}(k_x, k_y)$ of the HGB is given by

$$(3) \qquad \widetilde{F}(k_x, k_y) = \frac{1}{2\pi} \iint_{-\infty}^{+\infty} f_{l,m}(x,y) \exp(-ik_x x - ik_y y)\, dx\, dy.$$

In order to calculate the Fourier transformation, we use the following result

$$(4) \qquad \widetilde{F}\left[\exp(-x^2/2)H_n(x)\right] = (-i)^n \exp(-k^2/2)H_n(k),$$

which can be found in [9]. Its physical meaning is that Gaussian functions (for $l = m = 0$) have Gaussian spectra, and HGBs have Hermite–Gaussian spectra. In this way we obtain

$$(5) \quad \widetilde{F}(k_x, k_y) = \sqrt{\frac{C(l,m)\omega^2(z)}{2\pi}} (-i)^{l+m} \exp\left[\frac{-(k_x^2+k_y^2)\omega^2}{4}\right]$$
$$\times H_l\left(\frac{k_x\omega(z)}{\sqrt{2}}\right) H_m\left(\frac{k_y\omega(z)}{\sqrt{2}}\right).$$

As a next step we have to calculate

$$(6) \qquad \langle k_x^2 \rangle = \iint_{-\infty}^{+\infty} k_x^2 |\widetilde{F}(k_x, k_y)|^2\, dk_x\, dk_y.$$

Simplifying Eq. 6 as a product of two integrals and using again the orthogonality relation between the Hermite polynomials

$$(7) \qquad \langle k_x^2 \rangle = \frac{2^m m!}{\sqrt{2\pi}} C(l,m)\omega(z) \int_{-\infty}^{+\infty} k_x^2 \exp\left[-\frac{k_x^2\omega^2(z)}{2}\right] H_l^2\left(\frac{k_x\omega(z)}{\sqrt{2}}\right) dk_x.$$

A useful relation is that $\int_{-\infty}^{+\infty} \exp(-\xi^2)H_l^2(\xi)\xi^2\, d\xi = \sqrt{\pi}2^l l!(l+\frac{1}{2})$. In our case $\xi \equiv k_x\omega(z)/\sqrt{2}$. In this way we get

$$(8) \qquad \langle k_x^2 \rangle = \frac{2l+1}{\omega^2(z)} C(l,m)2^m m! 2^l l! = \frac{2l+1}{\omega^2(z)}.$$

L. Stoyanov, N. Gorunski, M. Mincheva et al.

Because of the symmetry, $\langle k_y^2 \rangle = (2m+1)/\omega^2(z)$. Finally, let us calculate the Gouy phase Φ_G (see Eq. 1) by splitting it into two parts ($\Phi_G = \Phi_{G1} + \Phi_{G2}$). For Φ_{G1} we obtain

$$(9) \qquad \Phi_{G1} = -\frac{2l+1}{k} \int \frac{dz}{\omega_0^2\left[1 + (z/z_R)^2\right]} = -\left(l + \frac{1}{2}\right) \arctan(z/z_R).$$

Because of the symmetry of the mode indices l and m, we get directly $\Phi_{G2} = -\left(m + \frac{1}{2}\right)\arctan(z/z_R)$. In this way, the total Gouy phase of a HGB with mode indices l and m is

$$(10) \qquad \Phi_G = -(1 + l + m)\arctan(z/z_R),$$

where the Rayleigh diffraction range $z_R = \pi\omega_0^2/\lambda$ is related to the beam width $\omega_0 = \omega(z=0)$ at its waist and to the wavelength λ.

3. Experimental results and discussion. Let us first describe the single-lens interferometer, which is probably the simplest interferometer [10]. The only required optical element is a focusing lens with no antireflection coatings. If so, after two Fresnel reflections from its surfaces (see points marked with 1 and 2 in Fig. 1(a)), a strongly converging "ghost" beam is formed. This "ghost" beam is co-axial with respect to the main "background" beam and its secondary focal plane is much closer to the lens than its usual focal plane. The paraxial model presented in [11] (see Eq. (9)) shows that the distance f_{eff} from the lens to the "ghost" beam waist is related to the focal length f of the lens by $f_{\text{eff}} = f(n-1)/(3n-1)$, where n is the refractive index of the used glass. As expected, the secondarily reflected beam has much lower intensity than the background beam. However, in the "ghost" beam focal region its intensity is high, ensuring an excellent modulation
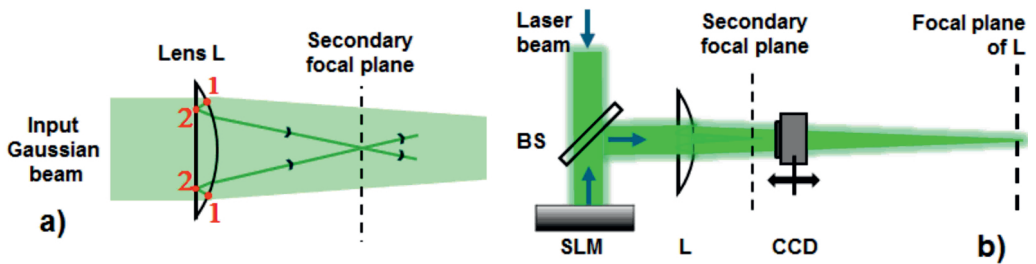

Fig. 1. Principle of operation of the single-lens interferometer (a) and used experimental setup (b). In panel (a), the reflection of the background Gaussian beam is depicted inside the lens by dots and numbers, showing the formation of the "ghost" beam. The arrows mark the propagation direction of the "ghost" beam. In panel (b) the vertical dashed lines mark the usual focal plane of the lens (right) and the secondary focal plane of the "ghost" beam (left). Panel (b): cw laser emitting at 532 nm SLM – liquid crystal spatial light modulator. BS – beam splitter. L – uncoated focusing lens ($f = 100\,\text{cm}$). CCD – charge-coupled device camera mounted on a translation stage

C. R. Acad. Bulg. Sci., **77**, No 8, 2024

1141

depth of the interference pattern with the slightly converging background beam. The range of existence of this pattern is, however, short (of the order of units of centimetres, depending on the focal length of the lens L).

In the experiment, the charge-coupled device camera (CCD) is mounted on a translation rail. In this manner, we are able to record Gouy-phase-dependent interference patterns at different propagation distances. At each position, the CCD camera captures an interferogram. From each interferogram we evaluate the intensity in the centre of the interference pattern. The sequence of data we will further denote as axial interference signal. One such signal for the Hermite–Gaussian mode HG_{42} (normalized to unity) is presented in the left graph of Fig. 2 with hollow circles. In the three frames between the graphs in Fig. 2, we show the essential parts of the interferograms recorded in the secondary focal plane (A), at the first on-axis minimum (B) and at the first side-lying maximum (C) of the interference signal. The arrows indicate the approximate axial region from which, frame by frame, the experimental points are extracted (see the left plot of Fig. 2; hollow circles). We intentionally show the data for this HG_{42} mode, since, in this case the deviations of the experimental data from the theoretical prediction are the largest.

The applied operations for processing the experimental data are as follows:

i) Subtraction of a reference line from the recorded axial interference signal to take into account the change of the beams' intensities. Normalization of the experimental data;

ii) Approximation of the normalized interference signal with a function of the type $g(z) = E + F \cos[(1 + l + m) \arctan(z/z_R) + G]/H$, where z is the longitudinal coordinate and E, F, G, H are fit parameters;

iii) Apply $\arccos\{\cos[\ldots]\}$ in order to transfer the obtained approximation of the experimental data to the range $[-\pi, \pi]$. If necessary (for higher-order HG-modes), unfold the obtained approximation for the phase to a multiple of π.

iv) Apply arccos-function to the experimental data and repeat the procedure in the preceding point.

The result obtained by following the described procedure for mode HG_{42}, is shown in the right graph of Fig. 2. Hollow circles denote the processed experimental data, while the solid curve presents the processed fit curve. The asymptotic theoretical value of the Gouy phase for this HG_{42} mode is $(1+4+2)\pi/2 = 7\pi/2$. It can be seen that the curve approximating the data tends towards this value but does not reach it at the maximal accessible distance of $5\,\mathrm{cm}$ from the focus. The experimental data, although showing the same trend, saturate at shorter propagation distance and differ from the asymptotic value by 12%. This is the case
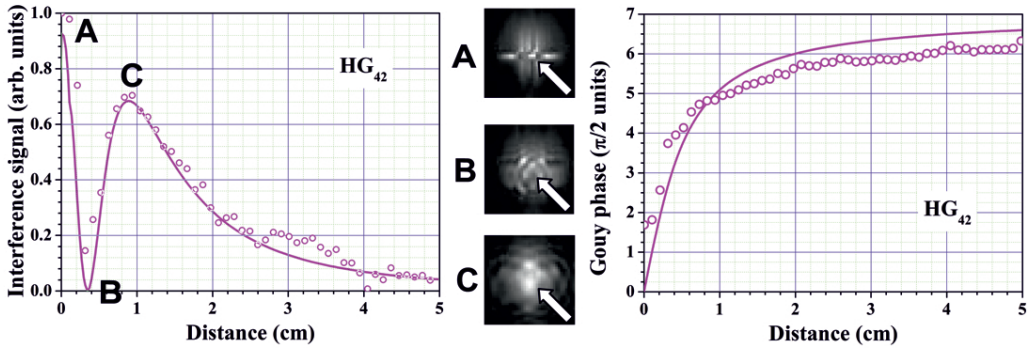
L. Stoyanov, N. Gorunski, M. Mincheva et al.

Fig. 2. Left: Normalized interference signal (hollow circles) obtained with a HG_{42} mode and the central part of the background beam and interpolation curve (solid curve) of the type $g(z) = E + F \cos[(1 + l + m) \arctan(z/z_R) + G]/H$ with E=0.344, F=0.34, G=-1.4 rad, H=0.9, and z_R=0.43 cm for l=4 and m=2. Middle: Experimentally recorded interference patterns in the secondary focal plane (A), at the first on-axis minimum (B) and at the first side-lying maximum (C) of the interference signal. Right: Gouy phase reconstructed from the experimental data (open circles) and theoretical result (solid curve), both presented in $\pi/2$ units

with the largest deviation between the asymptotic experimental and theoretical values we report here.

Figure 3 summarizes the results obtained for the Gouy phase for five different modes (the fundamental Gaussian mode HG_{00} and even higher-order HG modes
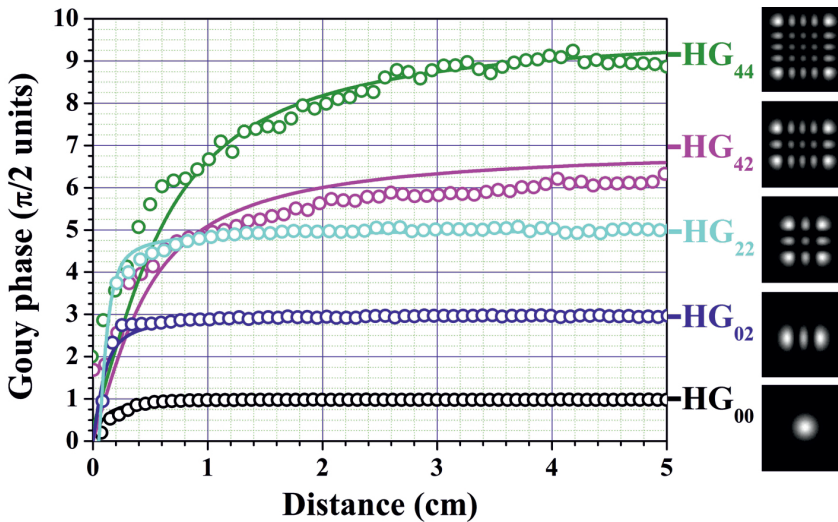

Fig. 3. Gouy phases (in $\pi/2$ units) for five symmetrical HG modes vs. propagation distance from the secondary focal plane. Hollow circles – data retrieved from the experiment. Solid curves – theoretical approximations. Horizontal bars on the right, outside the graph – theoretical asymptotic value for the respective HG_{lm} mode. Greyscale frames – calculated intensity distributions of the HG modes

HG_{lm}, $l, m = 0, 2, 4$). It is worth underlining that only symmetric HG modes, e.g., with a bright central sub-peak along the beam axis, are studied. Thus, the interference signals with the "ghost" beams are obtained exactly along the propagation axis of the modes and, in this sense, the experiments correspond exactly to the definition of the Gouy phase. (This would not be the case, for example, with the HG_{01} mode in which there are two bright sub-beams separated by a one-dimensional phase dislocation along the propagation axis of the mode where the intensity drops down to zero. In this case, there will be no interference signal, thus the "ghost" beam must be shifted to overlap with one of the sub-peaks to obtain signal. This leads in turn to an additional phase in the measurement.)

In Fig. 3, the processed experimental data for the Gouy phase are represented by coloured hollow circles. The corresponding theoretical curves ($\Phi_G = (1 + l + m) \arctan(z/L_D)$) are represented by solid curves. The asymptotic values of the Gouy phase in the respective case are denoted with horizontal bars outside the plot area (on the left side of the mode labels). For modes $HG_{00,02,22}$ the data reach these asymptotic values within the exploited 5-cm range. For mode HG_{42}, as discussed above, the data reaches lower asymptotic value. For the highest mode HG_{44} investigated here, the asymptotic value is reached as well, however, the data are relatively noisier as compared to the other cases. In view of this, we can state that the presented results are in very good quantitative agreement with the theoretical dependence of the Gouy phase on the transverse mode indices of zeroth- and higher-order Hermite–Gaussian beams.

4. Conclusion. In this work, using a single-lens interferometer and a reflective spatial light modulator, we measured the Gouy phase shifts around the beam foci of higher-order Hermite–Gaussian modes HG_{lm} with transverse mode indices $l, m = 0, 2, 4$. To the best of our knowledge, these results constitute the first experimental verification of the analytical expression for the Gouy phase of these higher-order modes. The reported results are in very good quantitative agreement with the theory.

REFERENCES

[1] LINFOOT E. H., E. WOLF (1956) Phase distribution near focus in an aberration-free diffraction image, Proc. Phys. Soc. London, Sect. B, **69**(8), 823–832.
[2] FENG S., H. G. WINFUL (2001) Physical origin of the Gouy phase shift, Opt. Lett., **26**(8), 485–487.
[3] BOYD R. W. (2008) Nonlinear Optics (Third Edition), Academic Press.
[4] LASTZKA N., R. SCHNABEL (2007) The Gouy phase shift in nonlinear interactions of waves, Opt. Express, **15**(12), 7211–7217.
[5] LINDNER F., G. G. PAULUS, H. WALTHER et al. (2004) Gouy phase shift for few-cycle laser pulses, Phys. Rev. Lett., **92**(11), 113001.

L. Stoyanov, N. Gorunski, M. Mincheva et al.

[6] GHOMASHI B., R. REIFF, A. BECKER (2021) Coherence in macroscopic high harmonic generation for spatial focal phase distributions of monochromatic and broadband Gaussian laser pulses, Opt. Express, **29**(24), 40146–40160.

[7] SVELTO O. (2010) Principles of Lasers (Fifth Edition) Springer.

[8] ALLEN L., M. W. BEIJERSBERGEN, R. J. C. SPREEUW, J. P. WOERDMAN (1992) Orbital angular momentum of light and the transformation of Laguerre–Gaussian laser modes, Phys. Rev. A, **45**, 8185–8189.

[9] https://en.wikipedia.org/wiki/Hermite_polynomials

[10] MUNJAL P., K. P. SINGH (2019) A single-lens universal interferometer: Towards a class of frugal optical devices, Appl. Phys. Lett., **115**(11), 111102.

[11] PEATROSS J., M. V. PACK (2001) Visual introduction to Gaussian beams using a single lens as an interferometer, Am. J. Phys., **69**(11), 1169–1172.

Department of Quantum Electronics, Faculty of Physics, Sofia University "St. Kliment Ohridski", 5 J. Bourchier Blvd, 1164 Sofia, Bulgaria
e-mails: l.stoyanov@phys.uni-sofia.bg, naskog@phys.uni-sofia.bg, mariatm@uni-sofia.bg, pdrenkov@uni-sofia.bg, eelazarov@uni-sofia.bg, ald@phys.uni-sofia.bg